

Phase-space analysis of double ionization

Manfred Lein,^{1,2} Volker Engel,¹ E. K. U. Gross²

¹*Institut für Physikalische Chemie, Universität Würzburg,
D-97074 Würzburg, Germany*

voen@phys-chemie.uni-wuerzburg.de

<http://www.phys-chemie.uni-wuerzburg.de/engel/english.html>

²*Institut für Theoretische Physik, Universität Würzburg,
D-97074 Würzburg, Germany*

gross@physik.uni-wuerzburg.de

<http://theorie.physik.uni-wuerzburg.de/TP1/gross>

Abstract: We use the Wigner transformation to study the electronic center-of-mass motion in phase-space for double ionization in a strong laser field. The rescattering mechanism is clearly visible in the evolution of the fully correlated two-electron system. In a mean-field calculation, on the other hand, the signatures of rescattering are missing. Some properties of the Wigner function in two-particle systems are reported.

© 2001 Optical Society of America

OCIS codes: (270.6620) Strong-field processes; (020.4180) Multiphoton processes; (260.5210) Photoionization

References and links

1. D. N. Fittinghoff, P. R. Bolton, B. Chang, and K. C. Kulander, "Observation of Nonsequential Double Ionization of Helium with Optical Tunneling," *Phys. Rev. Lett.* **69**, 2642 (1992).
2. B. Walker, B. Sheehy, L. F. DiMauro, P. Agostini, K. J. Schafer, and K. C. Kulander, "Precision measurement of strong field double ionization of helium," *Phys. Rev. Lett.* **73**, 1227 (1994).
3. A. Becker and F. H. M. Faisal, "Mechanism of laser-induced double ionization of helium," *J. Phys. B* **29**, L197 (1996).
4. D. Bauer, "Two-dimensional, two-electron model atom in a laser pulse: Exact treatment, single-active-electron analysis, time-dependent density-functional theory, classical calculations, and non-sequential ionization," *Phys. Rev. A* **56**, 3028 (1997).
5. J. B. Watson, A. Sanpera, D. G. Lappas, P. L. Knight, and K. Burnett, "Nonsequential Double Ionization of Helium," *Phys. Rev. Lett.* **78**, 1884 (1997).
6. D. G. Lappas and R. van Leeuwen, "Electron correlation effects in the double ionization of He," *J. Phys. B* **31**, L249 (1998).
7. W.-C. Liu, J. H. Eberly, S. L. Haan, and R. Grobe, "Correlation Effects in Two-Electron Model Atoms in Intense Laser Fields," *Phys. Rev. Lett.* **83**, 520 (1999).
8. D. Dundas, K. T. Taylor, J. S. Parker, and E. S. Smyth, "Double-ionization dynamics of laser-driven helium," *J. Phys. B* **32**, L231 (1999).
9. M. Lein, E. K. U. Gross, and V. Engel, "On the mechanism of strong-field double photoionization in the helium atom," *J. Phys. B* **33**, 433 (2000).
10. M. Dörr, "Double ionization in a one-cycle laser pulse," *Opt. Express* **6**, 111 (2000), <http://www.opticsexpress.org/oearchive/source/19114.htm>.
11. Th. Weber *et al.*, "Recoil-Ion Momentum Distributions for Single and Double Ionization of Helium in Strong Laser Fields," *Phys. Rev. Lett.* **84**, 443 (2000).
12. R. Moshhammer *et al.*, "Momentum Distributions of Neⁿ⁺ Ions Created by an Intense Ultrashort Laser Pulse," *Phys. Rev. Lett.* **84**, 447 (2000).
13. Th. Weber *et al.*, "Sequential and nonsequential contributions to double ionization in strong laser fields," *J. Phys. B* **33**, L127 (2000).
14. Th. Weber *et al.*, "Correlated electron emission in multiphoton double ionization," *Nature (London)* **405**, 658 (2000).
15. A. Becker and F. H. M. Faisal, "Interpretation of momentum distribution of recoil ions from laser induced nonsequential double ionization," *Phys. Rev. Lett.* **84**, 3456 (2000).

16. H. W. van der Hart, "Recollision model for double ionization of atoms in strong laser fields," *Phys. Rev. A* **62**, 013407 (2000).
 17. H. W. van der Hart, "Sequential versus non-sequential double ionization in strong laser fields," *J. Phys. B* **33**, L699 (2000).
 18. R. Kopold, W. Becker, H. Rottke, and W. Sandner, "Routes to Nonsequential Double Ionization," *Phys. Rev. Lett.* **85**, 3781 (2000).
 19. B. Feuerstein, R. Moshhammer, and J. Ullrich, "Nonsequential multiple ionization in intense laser pulses: interpretation of ion momentum distributions within the classical 'rescattering' model," *J. Phys. B* **33**, L823 (2000).
 20. M. Lein, E. K. U. Gross, and V. Engel, "Intense-Field Double Ionization of Helium: Identifying the Mechanism," *Phys. Rev. Lett.* **85**, 4707 (2000).
 21. J. Chen, J. Liu, L. B. Fu, and W. M. Zheng, "Interpretation of momentum distribution of recoil ions from laser-induced nonsequential double ionization by semiclassical rescattering model," *Phys. Rev. A* **63**, 011404(R) (2001).
 22. P. B. Corkum, "Plasma perspective on strong field multiphoton ionization," *Phys. Rev. Lett.* **71**, 1994 (1993).
 23. M. Hillery, R. F. O'Connell, M. O. Scully, and E. P. Wigner, "Distribution functions in physics: fundamentals," *Phys. Rep.* **106**, 121 (1984).
 24. R. Grobe and J. H. Eberly, "Single and double ionization and strong-field stabilization of a two-electron system," *Phys. Rev. A* **47**, R1605 (1993).
 25. M. D. Feit, J. A. Fleck, Jr., and A. Steiger, "Solution of the Schrödinger equation by a spectral method," *J. Comput. Phys.* **47**, 412 (1982).
-

1 Introduction

The discovery of the anomalously large double-ionization probabilities for laser-driven atoms [1, 2] initiated lively discussions about the mechanism of laser-induced multiple ionization. It was quickly accepted that the electron-electron correlation plays an important role in the process because it was not possible to reproduce the experimental findings within uncorrelated model calculations. The "knee structure" in the intensity dependence of the double-ionization yield indicated that a correlated "non-sequential" process dominates at lower intensities while uncorrelated "sequential" ionization takes over at higher intensities, for He at about $I \sim 10^{15}$ W/cm². Non-sequential double ionization was soon found in a number of calculations [3–10] using a variety of different approaches, but the physical picture has remained controversial until recently. A series of new experiments [11–14] and calculations [15–21] was initiated by measurements of the recoil-ion momentum spectra by Weber *et al.* [11] and Moshhammer *et al.* [12]. These are very much in favor of the rescattering picture [22]: After a first single-ionization step, the outer electron is accelerated by the laser and returns to the core where energy can be transferred to the second electron by recollision. In essence, this is a classical picture and classical dynamics is usually visualized in phase space. Hence, the most appropriate way to confirm that rescattering actually leads to double ionization is the inspection of the phase-space motion. In quantum mechanics, the distribution in phase-space is obtained via the Wigner transformation [23]. However, for a wave function depending on two coordinates, the Wigner function has already four dimensions, which is too many to be easily analyzed. Therefore, in order to study the phase-space dynamics of both electrons, we consider the dynamics of the electronic center-of-mass. Its momentum $P = p_1 + p_2$ is related to the recoil-ion momentum $p^{(2+)}$ by $P = -p^{(2+)}$ as a consequence of the approximate momentum conservation: The laser photons carry negligible momentum. Hence, the center-of-mass motion has a direct relation to the recoil-ion momentum distributions which have become very important in the experimental study of double ionization. In our previous work, we have shown that rescattering shows up clearly in the electronic center-of-mass phase-space motion [20]. In the present work we investigate the center-of-mass phase-space dynamics in more detail. For the one-dimensional model of the helium atom, we explore the exact time evolution and compare with the result

of a time-dependent Hartree-Fock (HF) calculation. We find that the typical signatures of rescattering are absent in the HF approach, showing that the mean-field level of electron-electron interaction cannot properly describe non-sequential double ionization. On the way we will encounter some interesting properties of the Wigner transformation.

2 Model

We use the 1D two-electron model atom with soft-core Coulomb potentials [24]. The length-gauge Hamiltonian in atomic units reads

$$H = -\frac{1}{2} \frac{\partial^2}{\partial z_1^2} - \frac{1}{2} \frac{\partial^2}{\partial z_2^2} - \frac{2}{\sqrt{z_1^2 + 1}} - \frac{2}{\sqrt{z_2^2 + 1}} + \frac{1}{\sqrt{(z_1 - z_2)^2 + 1}} + E(t)(z_1 + z_2). \quad (1)$$

Here, z_1 and z_2 are the electron coordinates along the direction of the laser polarization, and $E(t) = E_0 \sin \omega t$ is the electric field of the laser. The coordinates can assume positive and negative values, so that the electrons may pass by the nucleus. Numerically, we represent the time-dependent two-electron wave function $\Psi(z_1, z_2, t)$ on a two-dimensional grid extending at least 300 a.u. in each dimension. The separation between the grid points is 0.2 a.u. The initial state is the singlet ground state which we obtain by propagation of an arbitrary symmetric wave function in imaginary time. The time evolution under the influence of the laser field is calculated through numerical integration of the time-dependent Schrödinger equation, using the split-operator method [25] with 2000 time steps per optical cycle. At the grid boundary, an optical potential is added to the external potential to ensure that outgoing flux is absorbed rather than reflected from the boundary. The width of this absorbing mask is one tenth of the total grid size. For the results shown in this work, a 780 nm laser with intensity 10^{15} W/cm² is employed. The classical oscillation amplitude for these parameters is $\alpha = E_0/\omega^2 = 49$ a.u., i.e., the grid is large enough to account for recollision events. In our previous work, we have demonstrated [9] that the laser pulse shape does not play an important role for the ionization mechanism. Considering a certain time during the action of the pulse, single and double ionization depend only on the intensity at that time, no matter if the laser has been turned on smoothly or not. Therefore, when we investigate the ionization mechanism, we may switch on the laser without using an envelope function. This has the advantage that the observed processes are not clouded by superposition of the phase-space density with wave packets from ionization during previous optical cycles.

Besides the exact time evolution we will consider the time-dependent Hartree-Fock approximation. Our two-electron system remains in a singlet state for all times, so the HF wave function simply reads

$$\Psi^{\text{HF}}(z_1, z_2, t) = \varphi(z_1, t) \varphi(z_2, t). \quad (2)$$

The time evolution of the orbital φ is governed by the one-particle Schrödinger equation

$$i \frac{\partial}{\partial t} \varphi(z, t) = \left[-\frac{1}{2} \frac{\partial^2}{\partial z^2} + v_s(z, t) \right] \varphi(z, t), \quad (3)$$

with the single-particle potential v_s given by

$$v_s(z, t) = -\frac{2}{\sqrt{z^2 + 1}} + \int \frac{|\varphi(z', t)|^2}{\sqrt{(z - z')^2 + 1}} dz' + E(t) z. \quad (4)$$

3 The Wigner transformation for a two-electron system

The Wigner function corresponding to a one-particle wave function $\varphi(x)$ is given by

$$w^{(1)}(x, p) = \int \varphi^* \left(x - \frac{y}{2} \right) \varphi \left(x + \frac{y}{2} \right) e^{-ipy} dy. \quad (5)$$

This quantity is always real, but can be positive or negative. The integration of $w^{(1)}$ over the momentum p correctly yields the coordinate probability distribution $|\varphi(x)|^2$ (except for a prefactor 2π). Likewise, the integration over x yields the momentum distribution. Therefore, and despite the fact that the Wigner transform may assume negative values, it is usually interpreted as the probability distribution in the one-particle phase space spanned by the coordinate x and the momentum p .

For a many-body wave function such as $\Psi(z_1, z_2)$, the Wigner transformation may be carried out for *each* coordinate. The number of dimensions is thereby doubled. As in [20], we avoid the large number of dimensions by introducing the Wigner transformation with respect to the electronic center-of-mass coordinate $Z = (z_1 + z_2)/2$; we do not transform with respect to the relative coordinate $z = z_2 - z_1$:

$$w(Z, P, z) = \int \Psi^* \left(Z - \frac{y}{2} - \frac{z}{2}, Z - \frac{y}{2} + \frac{z}{2} \right) \Psi \left(Z + \frac{y}{2} - \frac{z}{2}, Z + \frac{y}{2} + \frac{z}{2} \right) e^{-iPy} dy. \quad (6)$$

Subsequently, we integrate over the relative coordinate z to obtain the phase-space distribution for the center of mass:

$$w(Z, P) = \int w(Z, P, z) dz. \quad (7)$$

Concerning the numerical evaluation of $w(Z, P)$, it is more efficient (yet equivalent) to first integrate over z and then carry out the Fourier transformation. In this way, we do not need to handle the complicated integrand in Eq. (6), which depends on four variables.

Below we will apply the phase-space analysis to a time-dependent HF calculation. In this case, the time-dependent wave function is a product wave function, see Eq. (2), and it is straightforward to prove that the center-of-mass phase-space distribution takes the simple form

$$w^{\text{HF}}(Z, P) = \frac{1}{2} \left[w^{(1)} \left(Z, \frac{P}{2} \right) \right]^2, \quad (8)$$

where $w^{(1)}(x, p)$ is the one-particle Wigner function as defined in Eq. (5). From Eq. (8) we see that w^{HF} exhibits some peculiarities. Obviously, $w^{\text{HF}}(Z, P)$ is always greater or equal to zero, contrary to a general Wigner function. This is a nice feature since it simplifies the interpretation. Consider now the case that $\varphi(x)$ is a superposition of two wave packets, centered at $x = \pm a$, i.e., $\varphi(x) = \varphi_a(x) + \varphi_{-a}(x)$. The Wigner function $w^{(1)}(x, p)$ then contains maxima at $x = \pm a$. Therefore, by Eq. (8), the two-particle quantity $w^{\text{HF}}(Z, P)$ contains maxima at $Z = \pm a$ as well, corresponding to the case where both electrons are located at $-a$ or where both electrons are located at $+a$. However, the HF wave function $\Psi^{\text{HF}}(z_1, z_2) = \varphi_a(z_1)\varphi_a(z_2) + \varphi_a(z_1)\varphi_{-a}(z_2) + \varphi_{-a}(z_1)\varphi_a(z_2) + \varphi_{-a}(z_1)\varphi_{-a}(z_2)$ also contains the possibility that the electrons are located on opposite sides, corresponding to phase-space density around $Z = 0$. By Eq. (8), the one-particle distribution then contains density at $x = 0$; thinking classically, this should not be the case. The solution to the paradox is that the one-particle distribution exhibits rapid oscillations between positive and negative values in the region at $x = 0$. These oscillations would average to zero if the Wigner function was convoluted with some smoothing window function. By applying the square in Eq. (8), we obtain a positive function which cannot average to zero.

We conclude this section by giving the generalization of the upper relation to a symmetrized/antisymmetrized product of two different one-particle wave functions φ_1, φ_2 ,

$$\Psi^{\text{s/a}}(z_1, z_2) = \varphi_1(z_1)\varphi_2(z_2) \pm \varphi_1(z_2)\varphi_2(z_1). \quad (9)$$

The center-of-mass phase-space density as defined by Eq. (7) then reads

$$w^{\text{s/a}}(Z, P) = \left| \int \varphi_2^* \left(Z + \frac{y}{2} \right) \varphi_1 \left(Z - \frac{y}{2} \right) e^{iPy/2} dy \right|^2 \pm w_{\varphi_1} \left(Z, \frac{P}{2} \right) w_{\varphi_2} \left(Z, \frac{P}{2} \right), \quad (10)$$

where w_{φ_1} and w_{φ_2} are the Wigner distributions for φ_1, φ_2 . The second term in Eq. (10) arises from the symmetrization of the wave function.

4 Results

The center-of-mass phase-space motion for the exact temporal evolution of the model system is shown in the animation Fig. 1. The second animation, Fig. 2, is the result of the HF calculation. The time covered by the movies is $3T/2$ where T is one optical cycle, and the still images in Figs. 1, 2 are the final frames at $t = 3T/2$. Both movies include audio tracks explaining the time-dependent processes. We look at the exact

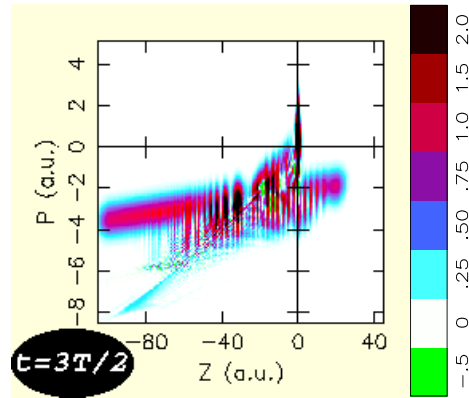


Fig. 1. (2.3 MB) The time evolution of the center-of-mass phase-space distribution.

calculation first. The system starts out from the ground state which, on the scale of our figures, has a narrow phase-space density around $Z = 0$ extending from about $P = -2$ a.u. to $P = +2$ a.u. In the first half optical cycle, the external electric field is positive so that the electrons are accelerated towards negative coordinates. At $t = T/2$, a very broad wave packet has appeared in the region $Z < 0$ and $P < 0$. Since double ionization is negligible during the first half cycle [9, 10], we can ascribe this density to pure single ionization. This is confirmed by the value of P at the lower end of the wave packet which agrees well with the maximum momentum that one electron can receive classically, namely the momentum after a half cycle of free acceleration in the electric field, $|P_{\text{max}}| = 2E_0/\omega = 5.8$ a.u. This means that the wave packet must be interpreted as one electron at $z = 2Z$ with momentum $p = P$, while the second electron remains close to $z = 0, p = 0$. Part of this density can return to the core after acceleration into the opposite direction during the second half cycle. When the electron collides with the core, i.e., when the density crosses the vertical axis $Z = 0$, we find that structures appear in the wave packet. See, e.g., the oscillations in $0 < Z < 20$ a.u., $3 \text{ a.u.} < P < 5$ a.u. at the time $t = T$. They are due to the superposition of scattered and unscattered density. At lower P we observe a strong second single-ionization wave packet. The fast oscillations for $Z > 20$ a.u. result from the overlap of the two single-ionization wave packets. The snapshot at $t = T$ clearly shows why the phase-space pictures are much more informative than snapshots in configuration or momentum space: There is very little overlap between the wave packets corresponding to ionization at different times; they can be clearly

separated. Projection either onto the Z or P axis would lead to considerable overlap, and we could not observe the time evolution of the individual wave packets. With increasing time, we find that tails evolve out of the scattered density. For $T < t < 3T/2$ the field accelerates the electrons towards negative coordinates. The tails are accelerated more strongly than the broad remainder of the wave-packet. A close examination reveals that the acceleration is about twice as large, indicating that this is density corresponding to two electrons freely accelerated by the laser. At $t = 3T/2$, the rescattering process is completed and the double-ionization wave packet at $(Z, P) \sim (-80, -7.5)$ a.u. has become essentially isolated from the rest. The ponderomotive momentum shift that the two electrons will receive when the laser field is adiabatically switched off amounts to $E_0/\omega = 2.9$ a.u. per electron. Therefore, a center-of-mass momentum of $P = -7.5$ a.u. at $t = 3T/2$ leads to a final recoil-ion momentum of $-(-7.5 \text{ a.u.} + 2 \times 2.9 \text{ a.u.}) = 1.7$ a.u.. This is in good agreement with experiment [11] and other calculations [15, 21]. Of course, rescattering will recur every half cycle. Also, multiple returns of the outer electron are possible, but no effect of multiple scattering can be distinguished in the movie.

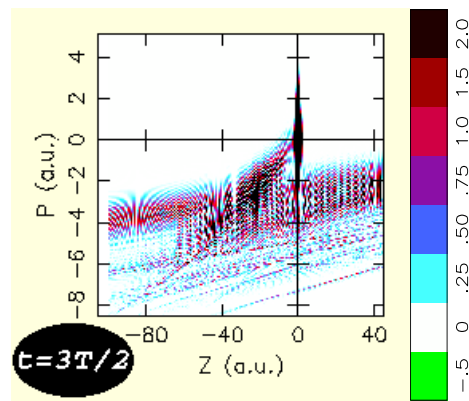


Fig. 2. (2.5 MB) Same as Fig. 1 in the Hartree-Fock approximation.

We compare now with the evolution of the system in the HF approximation, Fig. 2. From the beginning, there is a substructure in the phase-space density which was not present in the exact calculation. These oscillations are specific to the HF product wave function and have been discussed in Section 3. Apart from this effect, the observed wave packets are similar to the ones of Fig. 1. However, we find a long and thin double-ionization wave packet at $t = T/2$. This remarkable presence of uncorrelated ionization is consistent with [6], where it was found that at $I = 10^{15}$ W/cm², the HF double-ionization yield is already 1.4 times larger than the exact double-ionization yield. The most striking difference is that the single-ionization density does not suffer a noticeable change when it crosses $Z = 0$. I.e., rescattering does not affect the wave packet. Consistently, no tails corresponding to non-sequential double ionization appear within $T < t < 3T/2$, contrary to the exact calculation. Except for the density due to uncorrelated double ionization (mainly at $P < -5.5$ a.u.), all density at $t = 3T/2$ arises from single ionization.

We conclude that double ionization by rescattering only occurs in the fully correlated two-electron system, but is not found in the Hartree-Fock approach where the electron-electron interaction is included only at the mean-field level.

Acknowledgment

This work was supported by the Deutsche Forschungsgemeinschaft and the Fonds der Chemischen Industrie.